

Proof of Intercrystallite Ionic Transport in LiMPO_4 Electrodes ($M = \text{Fe, Mn}$)

Kyu Tae Lee, Wang H. Kan, and Linda F. Nazar*

University of Waterloo, Department of Chemistry, Waterloo, Ontario, Canada N2L 3G1

Received November 18, 2008; E-mail: lfnazar@uwaterloo.ca

Nanocrystallites have received much attention recently as potential electrode materials for energy storage owing to many factors. They have been shown to display different thermodynamic properties compared to bulk materials^{1,2} and to benefit from reduction in path length for carrier transport in materials such as LiMPO_4 ($M: \text{Fe, Mn, Co}$) which enhances their kinetic properties.^{3,4} However, many aspects of thermodynamics in nanosized LiMPO_4 materials are still not well understood, resulting in an imprecise understanding of the reaction mechanism of deintercalation/intercalation. There are at least three models proposed to explain the two-phase reaction of LiMPO_4 : shrinking core,⁵ platelet-type,^{6,7} and domino cascade.⁸ However, these models are not generally applicable to a “practical” nanocrystallite system containing a heterogeneous particle size distribution⁹ because they are based on characteristics dependent on morphology or homogeneity. Distinction between the models and determination of their validity can be complicated by these factors. Here, we show experimental evidence for a mechanism based on our proof of ionic transport between nano and bulk crystallites that results from their redox potential difference. This primarily originates from the dependence on thermodynamic properties on particle size as emphasized by Maier.¹

Homogeneously sized LiMPO_4 ($M: \text{Fe, Mn}$) nanorods and submicrometer-sized powders were synthesized to demonstrate the particle size effect on the thermodynamics of LiMPO_4 . For the nanocrystallites, 30 nm × 100 nm sized LiFePO_4 nanorods (Nano- LiFePO_4) and 40 nm × 200 nm sized LiMnPO_4 nanorods (Nano- LiMnPO_4) were synthesized by the modified polyol method,⁴ as shown in Figure 1c, e. To prepare “bulk” (*ca.* 500 nm) homogeneous LiMPO_4 crystallites (Bulk- LiMPO_4), we employed a solid-state method using a slight molar excess of Li and P. Heating the mixture at 600 °C under an N_2 atmosphere formed a two-phase [$\text{LiMPO}_4 + 0.1\text{Li}_3\text{PO}_4$] composite, which was treated with acetic acid to dissolve the Li_3PO_4 . A pure LiMPO_4 phase with a very narrow size distribution resulted, shown in Figure 1d, f (Figure S1: XRD patterns). This method resolves the problem of particle inhomogeneity that typically occurs in stoichiometric synthesis (Figure S2: SEM image).⁹

The redox potentials of Nano- $\text{Li}_{0.5}\text{FePO}_4$ and Bulk- $\text{Li}_{0.5}\text{FePO}_4$ demonstrate their different thermodynamic properties. The cells of Nano- and Bulk- LiFePO_4 were first fully charged and partially discharged to the composition $\text{Li}_{0.5}\text{FePO}_4$. For bulk particles, this corresponds to a two-phase mixture of ($\text{LiFePO}_4 + \text{FePO}_4$), whereas, for the nanocrystallites, we assume the end members are the partial solid solution phases ($\text{Li}_{1-\beta}\text{FePO}_4$ and $\text{Li}_\alpha\text{FePO}_4$ where $\beta \leq 0.89$, and $\alpha \geq 0.05$ as reported by Yamada et al.).¹⁰ The cells were held at an open circuit voltage (OCV) for 100 h to reach an equilibrium state. The resulting OCVs of Nano- $\text{Li}_{0.5}\text{FePO}_4$ and Bulk- $\text{Li}_{0.5}\text{FePO}_4$ are 3.428 and 3.420 V vs. Li/Li^+ , respectively. This difference is in accord with that predicted by Jamnik and Maier,¹¹ based on the rationale that particles of different sizes exhibit different chemical potentials. There also may be contributions to different surface energies that originate from the different

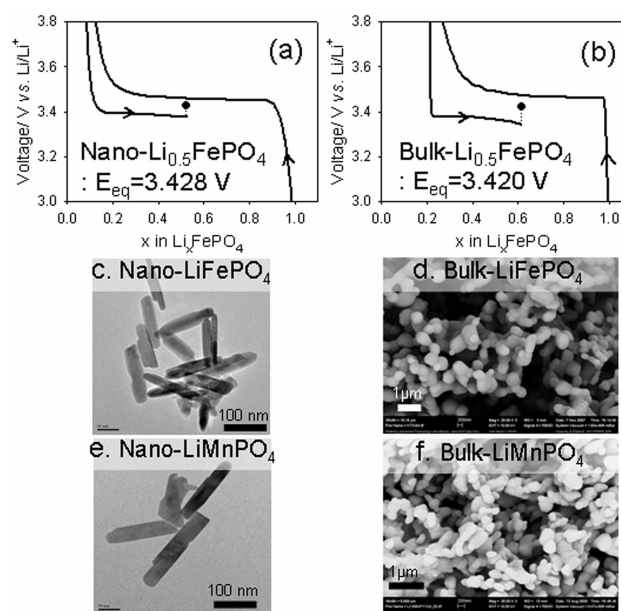


Figure 1. Relationship between thermodynamics and particle size. Electrochemical equilibrium potentials of (a) Nano- LiFePO_4 , (b) Bulk- LiFePO_4 . TEM images of (c) Nano- LiFePO_4 and (e) Nano- LiMnPO_4 . Representative SEM images of (d) Bulk- LiFePO_4 and (f) Bulk- LiMnPO_4 .

morphology of the nanocrystallites and bulk particles and/or the increased solubility limits of nanocrystallites. Recently, similar differences for OCVs for LiFePO_4 nanoparticles have been reported.¹² However, the implication of this on reaction mechanism has not yet been considered because of the small (*ca.* 10 mV) potential difference). We show here that it is significant.

To demonstrate this, Nano- FePO_4 (formed by chemical delithiation of Nano- LiFePO_4 ; Figure S3) was mixed with Bulk- LiFePO_4 in a 1:3 wt. ratio to maximize the contact area of the phases. The same was carried out for $\text{MnPO}_4/\text{LiMnPO}_4$. Composite electrodes were prepared with a mixture of phosphate (Nano- $\text{MPO}_4 + \text{Bulk-LiMPO}_4$), electrically conductive carbon (Super S), and poly(tetrafluoroethylene) (PTFE) binder in a 6:3:1 wt. ratio). The electrode was soaked in the electrolyte for 72 h to reach electrochemical equilibrium prior to assembling the cell. The XRD patterns of the electrodes before and after they were soaked in the electrolyte are compared in Figures 2 and S4. Before equilibration, the XRD reflections corresponding to LiMPO_4 display a narrow fwhm (full width at half-maximum, Figure 2a,b), in accord with the large crystallite size of the Bulk- LiMPO_4 phases. As clearly demonstrated for $M = \text{Fe}$ in Figure 2a, after electrochemical equilibration, the fwhm values of the LiFePO_4 phase increase to approach the fwhm characteristic of Nano- LiFePO_4 . This demonstrates that Nano- FePO_4 is lithiated to form Nano- LiFePO_4 , *via* ionic transport from Bulk- LiFePO_4 crystallites to the Nano- FePO_4 particles (Figure 3a.) The driving force is the difference in redox potential between them. In

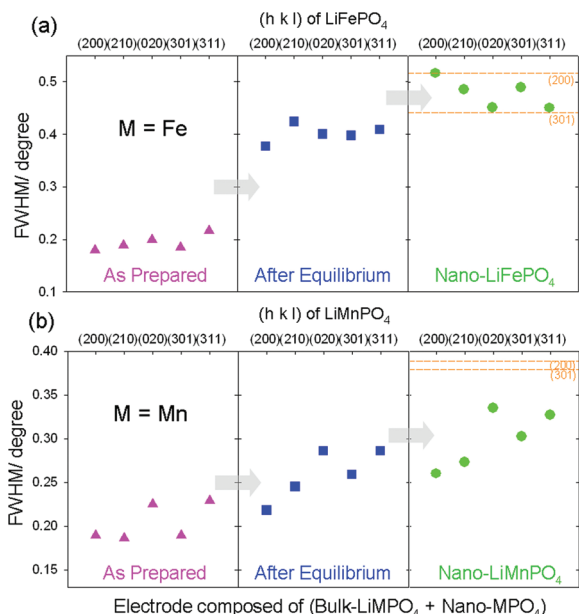


Figure 2. Proof of ionic transport. Fwhm values of XRD peaks corresponding to LiMPO_4 phases in electrode mixtures (Bulk- LiMPO_4 + Nano- MPO_4): (a) $M = \text{Fe}$ and (b) $M = \text{Mn}$. Dotted yellow lines correspond to the FWHM for the as-synthesized Nano- MPO_4 .

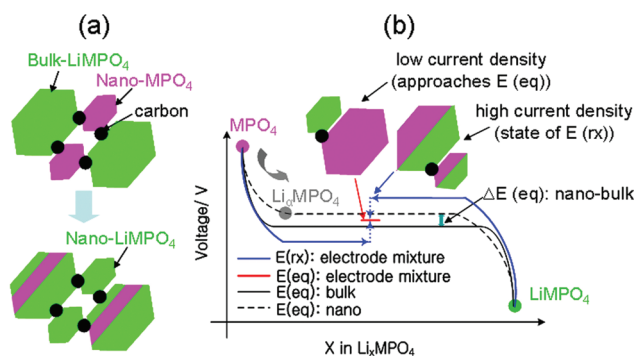


Figure 3. Schematic of the model; pink = MPO_4 ; green = LiMPO_4 .

the initial process, the potential of Nano- FePO_4 decreases to E_{eq} (Nano) by forming the solid solution phase Nano- $\text{Li}_\alpha\text{FePO}_4$, via transport of α Li from Bulk- LiFePO_4 (curved arrow Figure 3b). Note that α is ~ 0.088 as determined from the voltage profile in Figure 1a.¹³ Two distinct phases result because the solid-solution region of Bulk- LiFePO_4 is insignificant,¹⁰ as seen in the voltage profile of Figure 1b. Next, the ~ 10 mV ΔE_{eq} difference between Nano- $\text{Li}_\alpha\text{FePO}_4$ and Bulk- $\text{Li}_\alpha\text{FePO}_4$ in the two-phase reaction regime ($\alpha < x < 1-\beta$; cyan arrow, Figure 3b) drives the lithiation of Nano- $\text{Li}_\alpha\text{FePO}_4$ to Nano- LiFePO_4 . Concurrently, Bulk- LiFePO_4 is delithiated and forms Bulk- FePO_4 . Proof is the dramatic increase of the fwhm of the LiFePO_4 phase: otherwise, the fwhm would be similar before and after equilibrium. Exactly the same process is observed for LiMnPO_4 (Figure 2b). The increase in line width is very evident, albeit a little less dramatic owing to the well-known slower transport and equilibration in the Mn olivine. In summary, in the case of an electrochemical system with a heterogeneous particle size distribution (under low-intermediate current density), the smaller particles will be lithiated first—and the larger particles will be delithiated first—during charge and discharge in the region of $\alpha < x < 1-\beta$ in Li_xMPO_4 .

However, if a sufficiently high current is applied to the cell, it is probable that most particles will be two phase in nature because a high current will induce a large polarization. This is illustrated by the blue curve in Figure 3b. A higher (for delithiation) or lower (for lithiation) electrochemical potential than the E_{eq} of every particle would result. This is in accord with previous reports of two phases in a single particle by chemical delithiation via NOBF_4 or NO_2BF_4 .^{6,7} These oxidation potentials are much higher than either the equilibrium potentials of Nano- or Bulk- LiFePO_4 . Although particles formed at high current density will initially contain two phases within a single particle, nonetheless the equilibrium process will trigger the formation of one phase in a single particle (LiMPO_4 for smaller particles and MPO_4 for larger particles) after the cell is placed in open-circuit mode (dotted blue arrows, Figure 3b). This is pertinent to studies that utilize *ex situ* characterization methods to study phase distribution in LiMPO_4 crystallites. It may also shed light on some proposed mechanistic models. Redox potential differences may help to initiate spontaneous de/lithiation to form single-phase crystallites in an assembly of particle sizes that span down to the nanoregime.⁸

Simply considered, the electrochemical cell of crystallites with a heterogeneous particle size distribution is composed of the hierarchical structure of cathode (smaller particle) + anode (larger particle) inside a “practical” LiMPO_4 cathode. Thus, the current flow is more complex in the real electrochemical cell than in previously described models, because ionic transport between particles must be considered. This thermodynamic model can (and should) be applied to battery simulations for battery management systems (BMS), which is one of the key issues for the commercialization of electric vehicles.^{14,15} Furthermore, voltage profiles can be designed without changing the material composition. For an example, the typical flat profile of a two-phase olivine reaction would display a sloping profile similar to a solid-solution behavior by using an electrode comprised of crystallites having a wide but predictable particle size distribution.

Acknowledgment. NSERC is gratefully acknowledged for financial support.

Supporting Information Available: Data for synthesis details, XRD patterns, and SEM images. This material is available free of charge via the Internet at <http://pubs.acs.org>.

References

- (1) Maier, J. *Nat. Mater.* **2005**, *4*, 805.
- (2) Wagemaker, M.; Borghols, W. J. H.; Mulder, F. M. *J. Am. Chem. Soc.* **2007**, *129*, 4323.
- (3) Lim, S.; Yoon, C. S.; Cho, J. *Chem. Mater.* **2008**, *20*, 4560.
- (4) Kim, D. H.; Kim, J. *Electrochem. Solid-State Lett.* **2006**, *9*, A439.
- (5) Padhi, A. K.; Nanjundaswamy, K. S.; Goodenough, J. B. *J. Electrochem. Soc.* **1997**, *144*, 1188.
- (6) Chen, G.; Song, X.; Richardson, T. J. *Electrochem. Solid-State Lett.* **2006**, *9*, A295.
- (7) Laffont, L.; Delacourt, C.; Gibot, P.; Wu, M. Y.; Kooyman, P.; Masquelier, C.; Tarascon, J. M. *Chem. Mater.* **2006**, *18*, 5520.
- (8) Delmas, C.; Maccario, M.; Croguennec, L.; Le Cras, F.; Weill, F. *Nat. Mater.* **2008**, *7*, 665.
- (9) Striebel, K.; Shim, J.; Srinivasan, V.; Newman, J. *J. Electrochem. Soc.* **2005**, *152*, A664.
- (10) Yamada, A.; Koizumi, H.; Nishimura, S. I.; Sonoyama, N.; Kanno, R.; Yonemura, M.; Nakamura, T.; Kobayashi, Y. *Nat. Mater.* **2006**, *5*, 357.
- (11) Jamnik, J.; Maier, J. *Phys. Chem. Chem. Phys.* **2003**, *5*, 5215.
- (12) Meethong, N.; Huang, H. Y. S.; Carter, W. C.; Chiang, Y. M. *Electrochem. Solid-State Lett.* **2007**, *10*, A134.
- (13) Hence 3 mol% Bulk- LiFePO_4 (see Supporting Information for calculation) transforms to α Bulk- FePO_4 + $(1-\alpha)$ Bulk- LiFePO_4 .
- (14) Stewart, S. G.; Srinivasan, V.; Newman, J. *J. Electrochem. Soc.* **2008**, *155*, A664.
- (15) Snihir, I.; Rey, W.; Verbitskiy, E.; Belfadhel-Ayeb, A.; Notten, P. H. L. *J. Power Sources* **2006**, *159*, 1484.

JA8090559